Fibers and Polymers 2018, Vol.19, No.1, 11-21
DOI 10.1007/s12221-018-7768-5

ISSN 1229-9197 (print version)
ISSN 1875-0052 (electronic version)

Preparation and Characterization of A Semi-interpenetrating Network Alkaline Anion Exchange Membrane

Yifu Wang, Heting Wan, Dan Wang, Jilin Wang*, Lulu Wang, and Ruijiang Feng

School of Petroleum and Chemical Technology, College of Chemistry, Chemical Engineering and Environmental Engineering, Liaoning Shihua University, Fushun 113001, China

(Received September 6, 2017; Revised November 20, 2017; Accepted November 23, 2017)

Abstract: A series of semi-interpenetrating network (semi-IPN) anion exchange membranes (QCS/St-$G_{8\text{-}2\text{-}8}$, Quaternized chitosan/styrene-[maleic alkylene group diethyl bis (octyl dimethyl chloro/bromide), abbreviated as $G_{8\text{-}2\text{-}8}$] were prepared via in-situ polymerization by Styrene (St) and $G_{8\text{-}2\text{-}8}$ in QCS casting solution. During the process of in-situ polymerization, linear block polymers (St-$G_{8\text{-}2\text{-}8}$) of Styrene and $G_{8\text{-}2\text{-}8}$ was constructed, then was mixed with QCS casting solution, followed crosslinking the QCS by glutaraldehyde (GA). With the increasing content of linear block polymer, water uptake and swelling ratio of the composite membrane decreased; This kind of linear structure makes an order arrangement of quaternary ammonium groups which improves the OH^- migration efficiency. At 70 °C, the M-30 composite membrane performs a high OH^- conductivity of 8.20×10^{-2} $S\cdot cm^{-1}$, the methanol permeability is 3.23×10^{-6} $cm^{-2}\cdot s^{-1}$ which is still lower than Nafion 115 of 2.42×10^{-6} $cm^{-2}\cdot s^{-1}$, but M-30 shows a higher selectivity of 25.3 than Nafion 115 of 11.6. Furthermore, the membranes exhibited excellent thermal stability (≥150 °C), the tensile strength of the composite membrane is in the range of 14-25 MPa and elongation at break is in the range of 16-37 % at room temperature, as well as superior chemical stability in 1.0 M KOH solution for 250 h.

Keywords: Fuel cell, Ionic conductivity, Anion exchange membrane, Semi-interpenetrating

Introduction

Fuel cells are considered as the most promising electrochemical energy conversion devices for their high efficiency, high energy density and low pollution, which can be applied to mobile technology [1,2]. Of those, in the field of polymer electrolyte fuel cells including proton exchange membrane fuel cells (PEMFC) has attracted great attention in the past decades [3-5]. The most popular proton exchange membrane (PEM) currently used is Nafion, a sulfonated fluoropolymer highly efficient in proton conduction. However, their commercial development is still limited by the highly dependence on high-cost noble metal catalyst such as Pt and high fuel permeability [6]. Anion exchange membrane (AEM) based alkaline fuel cell (AFC) has been widely investigated due to advantages of faster fuel oxidation kinetics and improved oxygen reduction kinetics under alkaline condition. These would be applicable for using nonprecious metal catalysts such as Fe, Ni and Co, hence, greatly reducing the cost of fuel cell devices [7-9]. In addition, fuel permeability is sharply depressed since the OH^- migration is in the opposite direction to fuels [10].

As the key component of anion exchange membrane fuel cells (AEMFC), AEM serves as a conductor of OH^- and a barrier between oxidant and fuel. To date, most of AEMs have been prepared by introducing cationic groups such as quaternary ammonium [11,12], guanidinium [13,14], imidazolium [15,16], sulfonium [17], phosphonium [18,19] and metal ions [20,21] onto polymer backbones. In some of these strategies, carcinogenic reagent has once been used which is not green and sustainable. Although a variety of AEMs have been developed and great progresses have been made, the OH^- conductivity level is still lag behind PEMs and it is usually less than 1/4 of the H^+ conductivity of Nafion under the same ion exchange capacity (IEC, the amount of charge carriers in unit mass). This is due to the inherently lower mobility of OH^- ions (the mobility ratio between OH^- and H^+ is 0.57 in dilute aqueous solutions at room temperature) [22]. In fact, OH^- conductivity of AEM depends on two factors: mobility and IEC. It seems more easier to enhance OH^- conductivity by increasing IEC, but high IEC generally lead to excessive water uptake [23] and significant swelling ratio, especially at elevated temperatures [24,25], which are not good properties for AEMs. Hence, it is a more feasible and smarter strategy to increase OH^- conductivity by improving OH^- migration efficiency at a moderate IEC level.

In this work, the hydrophobic styrene monomer and Gemini surfactants [maleic alkylene group diethyl bis (octyl dimethyl chloro/bromide), abbreviated as $G_{8\text{-}2\text{-}8}$] were in situ polymerized in QCS matrix to form the linear block polymer, then the semi-interpenetrating network (semi-IPN) structure was constructed by dropwise adding the glutaraldehyde (GA) (as crosslinker) in the mixture of St-$G_{8\text{-}2\text{-}8}$ linear block polymers and QCS matrix solution. During the experiment, styrene was chosen as raw material due to its excellent mechanical properties and high thermal as well as chemical stability. It is worth to mentioning that the non-toxic $G_{8\text{-}2\text{-}8}$ surfactants is an excellent choice due to its special structure, such as possessing an unsaturated double bond for

*Corresponding author: wangjilin1978@163.com

polymerization and double quaternary ammonium groups to attract OH^-. The strategy offered in this work not only avoids the traditional chloromethylation approach to introduce quaternary ammonium groups onto polymer backbones, but also make an order arrangement of quaternary ammonium groups to achieve the OH^- directional migration. In addition, semi-IPN structure allows membrane to possess a dense structure and well mechanical properties. Besides, hydrophobic benzene rings and long alkyl chains also help to form the hydrophilic-hydrophobic microphase separation, improving OH^- migration efficiency, hence increasing OH^- conductivity.

Experimental

Materials

(2,3-epoxypropyl) trimethylammonium chloride (EPTMAC) was obtained from Shandong Dongying Guofeng Fine Chemicals Co., Ltd., $G_{8\text{-}2\text{-}8}$ Gemini surfactant purchased from Henan Daochun Chemical Technology Co., Ltd., and styrene obtained from Tianjin Damao Chemical Reagent Factory. The monomer styrene was pretreated with NaOH aqueous solution to remove the inhibitor before use. Chitosan (CS) (deacetylation degree is 95 %), Potassium persulfate (KPS), acetic acid, glutaraldehyde (GA) (50 wt%),

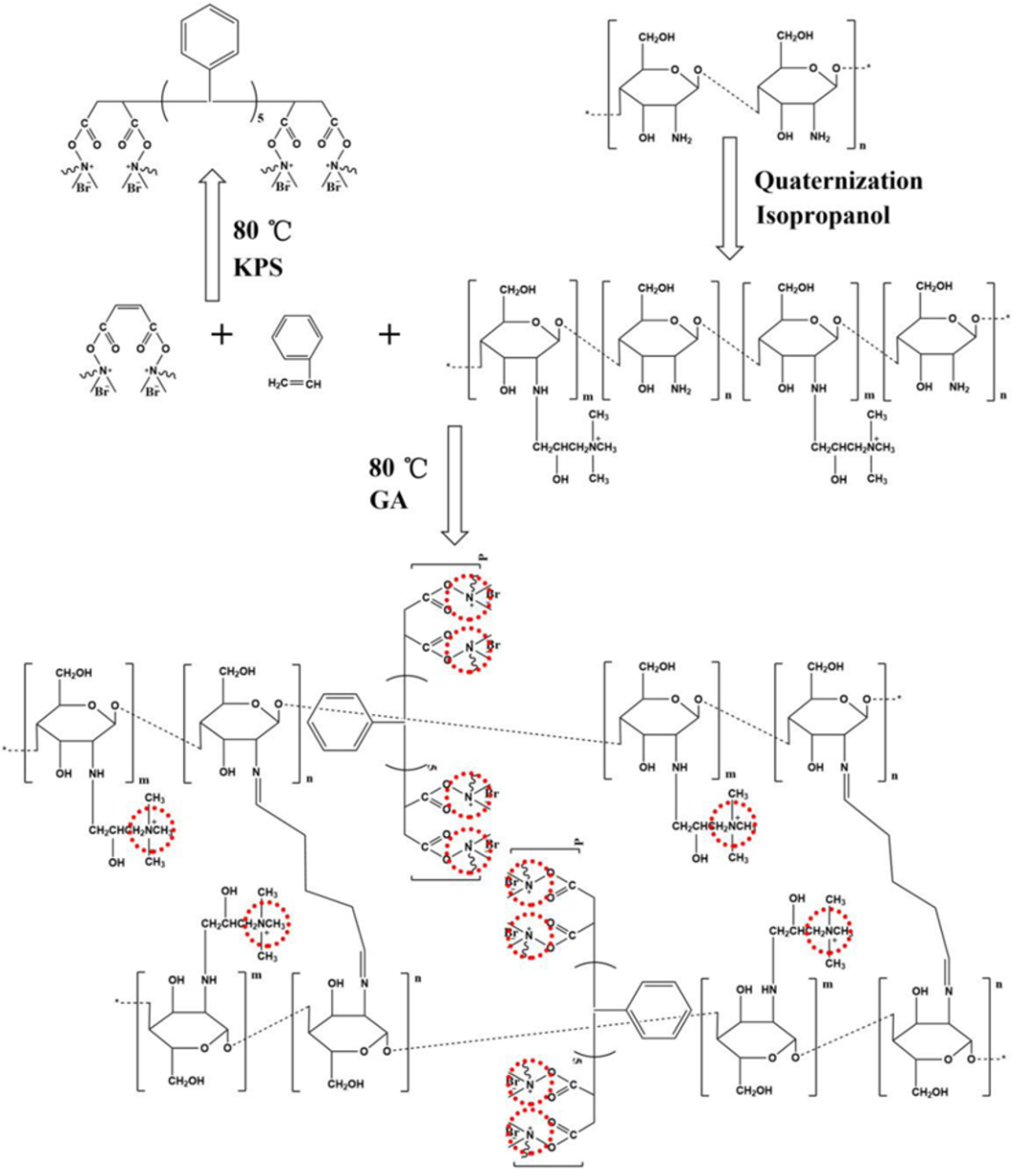

Scheme 1. Synthesis scheme of M-X (X=6, 12, 18, 24, 30) anion exchange membrane.

NaOH, isopropyl alcohol, hydrochloric acid (36-38 %), were all obtained from Sinopharm Chemical Reagent Co., Ltd. The reagents used were analytically grade. The deionized water was throughly used during the experiment.

The QCS in chloride form was synthesized by quaterinization of CS in isopropanol with EPTMAC at 85 °C for 10 h and it was afterwards isolated and purified according to the reference described elsewhere [26]. The degree of substitution (DS) of the QCS was 23.70 (±2.5) %, which was determined by titration with a standard $AgNO_3$ solution [27]. The same DS of QCS was here after used for all the membrane preparation.

Methods

Preparation of the QCS/St-$G_{8\text{-}2\text{-}8}$ Anion Exchange Membranes

2 g QCS dissolved in 2 % (v/v) acetate (20 m*l*), then a given amounts of $G_{8\text{-}2\text{-}8}$ and St (i.e.,$G_{8\text{-}2\text{-}8}$:St=1:5 in mole ratio) were added in above QCS casting solution and above resulting solution was copolymerized with KPS (0.5 % wt of the total weight) as a radical initiator (interval 1.5 h, added in three portions) at 80 °C for 6 h under continuous mechanical stirring. Then the crosslinked reaction was carried out for 20 min at 80 °C under the crosslinker (GA) (0.5 % wt) was added into the above solution and kept stirring. After cooling to room temperature, the resulted mixture containing QCS and St-$G_{8\text{-}2\text{-}8}$ block polymers were poured onto the glass plates to cast membranes. After evaporation of the solvent at room temperature, the obtained membranes were peeled off, then immersed into 1 M KOH aqueous solution for alkalization lasting for 48 h. At last the membranes were thoroughly washed with deionized water and then dried at 80 °C in vacuum oven until a constant weight. In this work, the anion exchange membranes were denoted as M-X, where X refers to the mass content of $G_{8\text{-}2\text{-}8}$ in the membranes and the weight percentage of $G_{8\text{-}2\text{-}8}$ (X) in the membrane is in the range of 0 %, 6 %, 12 %, 18 %, 24 % and 30 %. The schematic diagram of anion exchange membranes was seen in Scheme 1.

Instruments and Techniques

The FT-IR spectra of the membrane samples were recorded on a Perkin-Elmer Spectrum One (B) spectrometer (Perkin-Elmer, America) and all the samples were prepared as KBr pellets. The SEM images of the samples were taken with a SSX-550 scanning electron microscope (Shimadzu, Japan) by gold coating. Thermo gravimetric analysis (TGA) was performed on a TGA 290C analyzer (Netzsch Company, Germany) at a heating rate of 10 °C min^{-1} under N_2 atmosphere. The mechanical strength of the dry membranes was determined with an instrument CMT6502 (SANS Company, China). Dumbbell-shaped membrane samples of 25 mm×4 mm were prepared and the measurements were carried out by setting a constant separating speed of 5.00 mm min^{-1} under the ambient atmosphere. Tensile stress at break E was calculated by equation (1) [28].

$$E = \frac{F}{A_0} \tag{1}$$

where F is the applied force at break, A_0 is the initial cross-section area of the sample which is equal to $4\times L$ mm^2, and L is the thickness of the membrane.

Water Uptake and Swelling Ratio

The membrane samples were soaked in de-ionized water for various of time at room temperature to monitor the variations in weight and dimensions of the wet membranes. The weight and the dimensions of the wet membranes (P_{wet}) were measured rapidly after wiping the excessive surface water with a tissue paper, and those of the dry membranes (P_{dry}) were obtained by drying the samples at 60 °C in a vacuum oven until a constant weight was reached. The water uptake and swelling of the membranes were defined by equation (2):

$$\text{Water uptake (swelling) (\%)} = \frac{P_{wet} - P_{dry}}{P_{dry}} \times 100\% \tag{2}$$

Ion Exchange Capacity

The anion exchange membrane in hydroxide form was washed thoroughly with distilled water and then dried in a vacuum oven at 60 °C to reach a constant weight (w_{OH} in gram). It was afterwards immersed in a 0.1 mol l^{-1} HCl standard solutions at ambient temperature for 48 h under stirring to neutralize the hydroxide ions containing in the membrane. The mole number (equivalent) of the neutralized hydroxide ions (n) was determined by titration of the remanent acid with a 0.1 mol l^{-1} KOH standard solution. The ion exchange capacity (IEC) of the anion exchange membrane, termed as $\times 10^{-3}$ mol g^{-1} of hydroxide ions per gram of the dry hydroxide form membrane, was obtained by calculation from equation (3) [29].

$$IEC\ (\times 10^{-3}\ \text{mol g}^{-1}) = \frac{1000n}{w_{OH}} \tag{3}$$

OH^- Conductivity

OH^- conductivity measurement cell has been reported in our previous study [30,31]. The OH^- conductivity of the membrane was measured using alternating current (AC) with a frequency of 2 kHz supplied via a pair of platinum electrodes. Resistance between the two electrodes was evaluated with and without the membrane, respectively, to obtain the resistance of the membrane (R_M) by comparing the difference. In order to keep the electrodes were held at a fixed distance apart under the without membrane, the mini-gasket was used to cover the distance, which presents the thickness of the membrane. As discussed in our previous work [30], a lower concentration of the 0.1 mol l^{-1} KOH was employed as the electrolyte because a higher concentration of the KOH might affect the OH^- conductivity especially at higher temperatures, although the contribution of the KOH electrolyte has been subtracted. The OH^- conductivity (σ) of

the membrane was calculated by equation (4).

$$\sigma\,(\mathrm{S\ cm^{-1}}) = \frac{l}{R_M \times S} \quad (4)$$

where l is the thickness of the wet membrane (cm); and S is the membrane surface (cm^2) for ion transport, respectively. The temperature is controlled by putting the conductivity measurement cell in an oven.

Methanol Permeability

The methanol permeability of the composite membranes were determined at room temperature using a home-made diffusion cell comprising two compartments. In order to ensure the uniformity during the experiments, magnetic stirrers were used in each compartment. The membrane was clamped between the two compartments. One compartment was loaded with 1 M methanol aqueous solution (compartment A) and the other with de-ionized water (compartment B). The methanol concentration in the compartment (B) by permeation at any time t (in second), i.e., C_B in $mmol \cdot l^{-1}$, was monitored using a gas chromatograph (GC-6820, Agilent, USA). The methanol permeability P ($cm^{-2} \cdot s^{-1}$) through the membrane was calculated by equation (5).

$$P = (L/A) \times C_B V_B / (A(C_A - C_B)t) \quad (5)$$

where A (cm^2) and L (cm) are the membrane area and thickness, respectively; C_A ($mmol \cdot l^{-1}$) is the initial concentration of the methanol in the compartment (A); V_B (ml) is the water volume in the compartment (B).

Alkaline Stability

Stability of the membrane in an alkaline medium was investigated by monitoring the conductivity of the membranes as a function of immersion time in KOH solutions [32,33]. Detail procedure was that the membranes was immersed in 1 M KOH aqueous solutions at room temperature for different intervals. They were later thoroughly washed with de-ionized water (to remove the excess potassium hydroxide) and immersed in de-ionized water for more than 24 h prior to the measurement of OH^- conductivity at 80 °C. To distinguish OH^- conductivity of the membrane treated in alkaline solution for 0 h and the composite membrane treated for different immersion time (>0 h), the former was designated σ_0, and the latter was designated σ_t. The σ_t/σ_0 ratios were recorded as a function of immersion time (in the alkaline solution).

Single Cell Performance

The performance of M-30 membrane was tested in a single cell that consisted of commercial electrodes, Pt-Ru/C (30 wt% Pt, 15 wt% Ru) for the anode and Pt/C (20 wt% Pt) for the cathode, provided by Johnson Matthey. The loading of Pt and Pt-Ru catalysts at the cathode and anode was 1.0 and 2.0 $mg \cdot cm^{-2}$, respectively. The obtained membrane/elecrodes assembly (MEA) was then set into a 5 cm^2 fuel cell for testing using a commercial fuel cell test system (Arbin Instrument Corporation). The single cell was tested at 30 and 80 °C by feeding 5 M KOH and 3 M ethanol solution to the anode at a flow rate of 1 m$l \cdot min^{-1}$ to provide three-phase boundary and sufficient OH^-, while the cathode was supplied with 0.2 MPa O_2.

Results and Discussion

FT-IR Spectra

The pristine chitosan (CS) membrane and M-X composite membranes were characterized by FT-IR. As shown in Figure 1, the absorption peak appearing at 1660 cm^{-1} was assigned to the C=O stretch vibration resulted from the residual acetyl in commercial CS and the absorption at 1590 cm^{-1} was attributed to the N-H bending vibration of the primary amine for CS [34]. It was also noted that the peak originally corresponding to the primary amine (1590 cm^{-1}) of CS disappeared, instead, a new peak at around 1640 cm^{-1} was observed for QCS and other M-X composite membranes, revealing that the transformation of primary amine to the secondary amine due to the quaternary reactions at $-NH_2$ sites on CS chains by EPTMAC. In addition, new absorption peak at 1480 cm^{-1} which originated from the bending vibration of C-H in trimethylammonium chloride group was observed, indicating the existence of the quaternary ammonium groups in QCS [35].

Particular, all M-X membranes showed absorption bands of C-H group on the benzene ring at 3030 cm^{-1}, carbonyl absorption bands at 1650 cm^{-1}, -COOR absorption peak at 1250 cm^{-1} and the absorbance of the peaks increased with the increasing content of the St-$G_{8\text{-}2\text{-}8}$ block polymers. The results confirmed that the block polymers of polystyrene and $G_{8\text{-}2\text{-}8}$ was formed and has been successfully introduced into

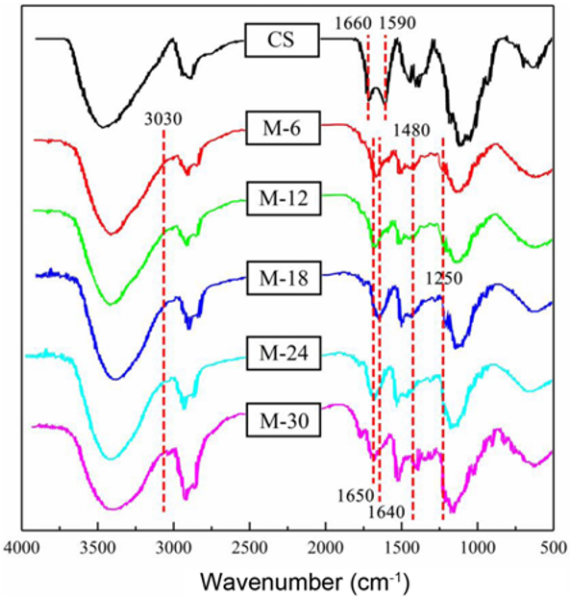

Figure 1. FT-IR spectra of CS and M-X (X=6, 12, 18, 24, 30) anion exchange membranes.

the membrane's structure.

Thermo-gravimetric Analysis (TGA) Studies

Thermal stability of AEMs is an important prerequisite for the use of fuel cells. Figure 2 presents the TGA curves of pristine QCS membrane and the M-X (X=6, 12, 18, 24, 30) membranes. A TGA curve of pristine QCS membrane shows two major mass loss regions. The first region at a temperature of 60-240 °C was due to the evaporation of free and bound water, of which the mass loss was about 5 %. The second transition region at around 210-360 °C was due to the degradation of quaternary ammonium groups in the QCS membrane. The total mass loss was about 70 % at 360 °C. However, The TGA curves of M-X (X=6, 12, 18, 24, 30) membranes also revealed two major mass loss regions, which appeared as a peak in the TGA curves. The first region at a temperature of 60-210 °C was also due to the evaporation of free and bound water. The peak of the second stage at around 210-360 °C was also due to the degradation of quaternary ammonium groups. Compared to the TGA of pristine QCS with of M-X membranes, it is found that the initial thermal decomposition temperature of the composite membrane decreased with the increasing content of $G_{8\text{-}2\text{-}8}$. It is due to the fact that more $G_{8\text{-}2\text{-}8}$ means more quaternized ammonium groups which are of lower decomposition temperature. Although the thermal stability of M-X membranes were lower than that of pristine QCS membrane, M-X membranes were found to be thermally stable up to 210 °C which can meet the application for fuel cells.

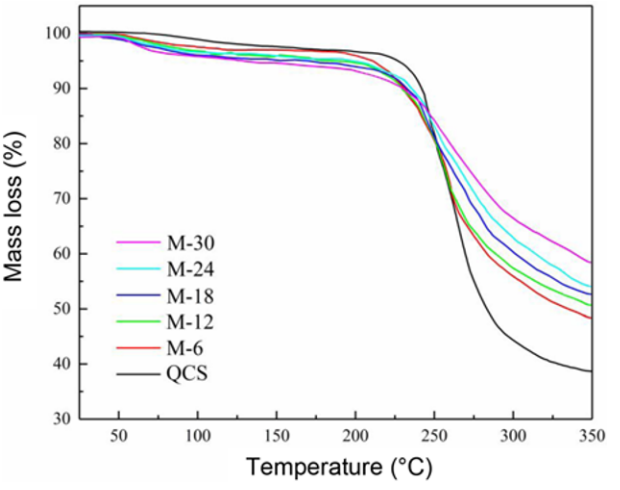

Figure 2. TGA curves of the QCS and M-X (X=6, 12, 18, 24, 30) anion exchange membranes at a heating rate 10 °C min^{-1} in N_2 atmosphere.

SEM

All the composite membranes prepared in this work are translucent with a pale yellow color. As can be seen in Figure 3, the surface morphologies of M-6 and M-30 composite membranes are smooth and flat with no cracks or any visible holes, the cross-sections of the membranes are uniform and dense indicating that the addition of $St\text{-}G_{8\text{-}2\text{-}8}$ block polymer didn't make a damage to membrane structure,

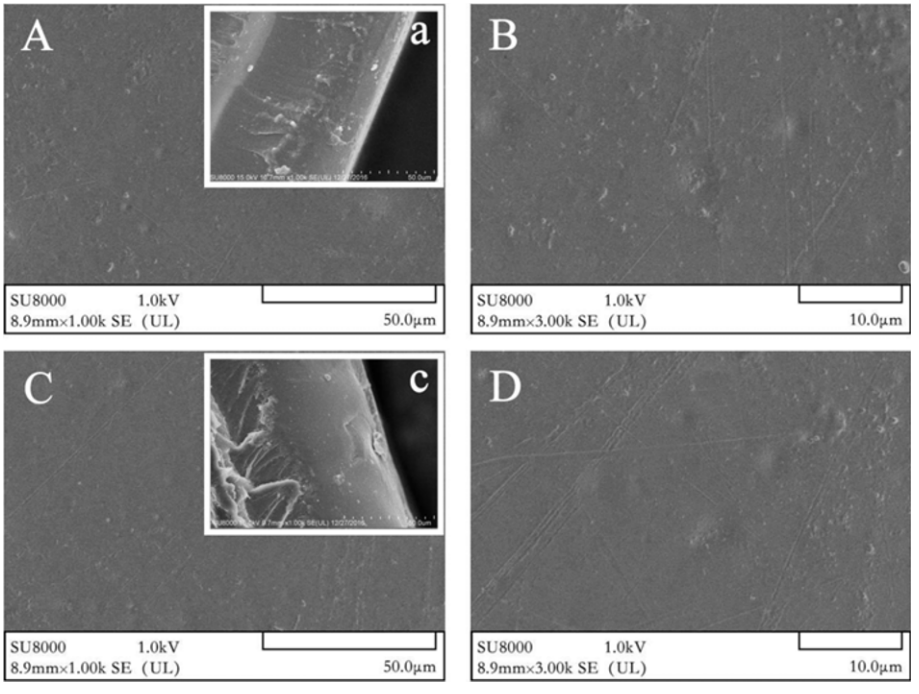

Figure 3. Surface and cross-section morphologies of the M-X (X=6, 30) anion exchange membranes; (A, B) in different magnification for M-6, (C, D) in different magnification for M-30, (a, c) are the cross-section morphologies for M-6 and M-30, respectivity.

instead, a good compatibility of QCS and St-$G_{8\text{-}2\text{-}8}$ block polymer was showed, which is essential for the membranes to maintain good mechanical properties and to improve alkaline stability.

IEC, Water Uptake, Swelling Ratio and Mechanical Property

Water uptakes, area swelling ratio of the composite membranes are closely related to IEC and mechanical properties [36]. Those are particularly important properties for fuel cell applications. Water uptake of the M-X (X=6, 12, 18, 24 and 30) membranes were showed in Figure 4 and the area swelling ratio, mechanical properties of the M-X membranes were summarized in Table 1. As seen from Table 1, the IEC value of the M-X membranes increased from 1.30×10^{-3} to 1.49×10^{-3} mol·g^{-1} with the increasing number of the quaternary ammonium groups grafted onto the chain of St-$G_{8\text{-}2\text{-}8}$ block polymers. As we all known that more quaternary ammonium groups will result in the higher water uptake and severe swelling ratio. Moreover, excessive water uptake and swelling ratio leads to an unacceptable dimensional change and loss of dimensional shape of the membrane, which increases the risk of mechanical weakness and dimensional mismatch, of the membrane was incorporated into a membrane electrode assembly.

However, in this work, both the water uptake and area swelling ratio of the M-X membranes decreased with the increasing content of St-$G_{8\text{-}2\text{-}8}$ block polymers, and that was due to the fact that the rigid structure of Styrene and Semi-interpenetrating network structure of the membranes can maintain the dimensional stability. Therefore, water uptake and area swelling ratio of the composite membranes are well controlled by adjusted the content of the St-$G_{8\text{-}2\text{-}8}$ block polymers in the composite membranes.

Apart from water uptake, swelling ratio are major concerns in the development of membranes [37]. The elongation at break and tensile strength of the M-X membrane were also showed in Table 1. The results revealed that the tensile strength and elongation at break generally increased with the increasing content of the block polymers. The reason for this was ascribed to the semi-IPN structure, the hydrophobic polystyrene and softened function of the quaternary ammonium groups. In this work, the crosslinked reaction has happened between the two QCS molecules. Thus, the chemical structure of the composite membranes will be more loosened, which was due to the QCS content decreased and St-$G_{8\text{-}2\text{-}8}$ block polymers content increased. However, the actual result was not aligned with the predicted result.

OH^- Conductivity and Apparent Activation Energy (Ea)

OH^- conductivities of M-X (X=6, 12, 18, 24 and 30) membranes at different temperatures were investigated. As can be seen in Figure 5, the OH^- conductivities of the composite membranes increased with the elevated temperature,

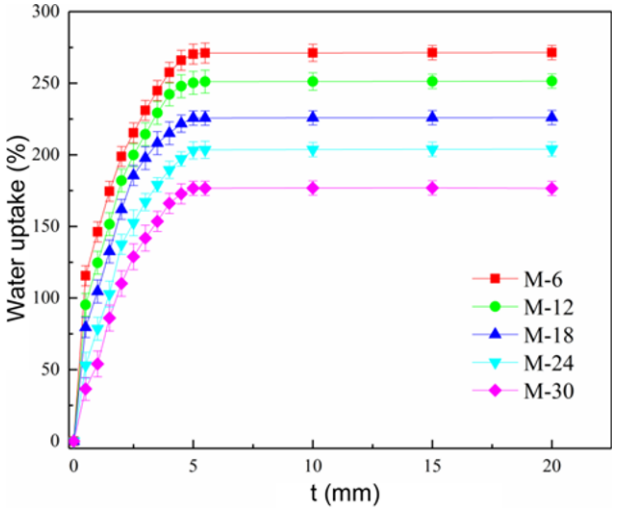

Figure 4. Water uptakes of the M-X (X=6, 12, 18, 24, 30) anion exchange membranes.

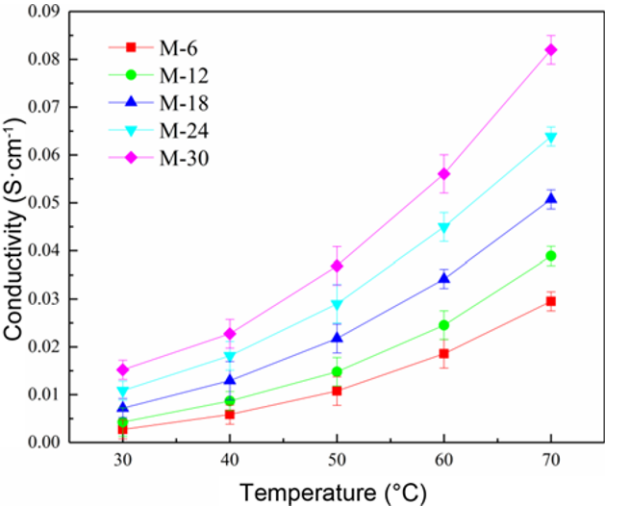

Figure 5. OH^- conductivity of M-X (X=6, 12, 18, 24, 30) anion exchange membranes.

Table 1. Properties of the M-X (X=6, 12, 18, 24, 30) anion exchange membranes

Membrane	M-6	M-12	M-18	M-24	M-30
SR (%)	172.00±5.20	156.00±3.10	125.00±3.00	96.00±1.25	69.00±2.20
TS (MPa)	14.14±0.11	17.25±0.21	20.47±0.23	23.98±0.31	25.34±0.24
Eb (%)	16.41±0.31	20.07±0.25	25.00±0.25	32.55±0.21	37.01±0.32

it was due to the fact that the mobility of OH^- were accelerated at higher temperature. M-30 membrane shows a higher OH^- conductivity of 8.2×10^{-2} S cm^{-1} at 70 °C than the values obtained by zeolite beta-filled chitosan membrane [38].

In this work, the content of quaternary ammonium groups in $G_{8\text{-}2\text{-}8}$ was increased with the increasing content of the St-$G_{8\text{-}2\text{-}8}$ block polymers. And those ionic groups, which were provided by QCS and $G_{8\text{-}2\text{-}8}$, could greatly enhance the OH^- conductivity of the M-X membranes. It is worth to mention that the linear block polymer can improve the effective migration of OH^- and boosts the OH^- conductivity of the anion exchange membrane with low IEC. Similar result was also found in the literature [39].

Table 2 lists the OH^- conductivities, IEC values and Conductivity/IEC values of various types of anion exchange membranes at similar temperatures. It can be seen from Table 2, the composite membrane (M-6 and M-30) prepared in this work shows a higher Conductivity/IEC values than those of membrane reported in literatures. It is due to the fact that linear block polymers make an orderly arrangement of cationic groups which could reduce the resistance of OH^- migration, increase the OH^- migration efficiency leading to a higher Conductivity/IEC values.

The activation energy (Ea) of the membrane for OH^- conduction was calculated according to the slope of the Arrhenius plots, and the results were indicated in Figure 6. With the decrease of QCS content, the activation energy decreased and the influence of the temperature on the activation energy was negligible. The value of the activation energy nearly keep constant with the increasing content of the St-$G_{8\text{-}2\text{-}8}$ block polymer, and that maybe result from the chemical structure was not nearly changed at the St-$G_{8\text{-}2\text{-}8}$ block polymer was introduced into the composite membranes. In fact, the chemical structure of the composite membranes will be more loosened, which was due to the decreased content of QCS and the increased content of St-$G_{8\text{-}2\text{-}8}$ block polymer. The crosslinked reaction has happened between the two QCS molecules. As we all learned that the more compact and rigid structure will result in lower free water contained in the membranes. On the contrary, the result will

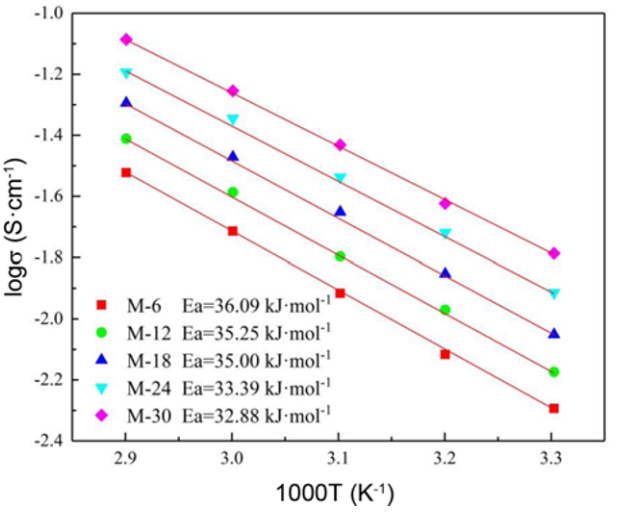

Figure 6. Arrhenius plots for the M-X (X=6, 12, 18, 24, 30) anion exchange membranes.

tend to the opposite. In this work, the more free water will be contained into the composite membranes and the OH^- conductivity should also be increased, which was proved by the measure result of conductivity.

According to vehicle mechanism [47] the free water can act as a carrying medium. In this work, the activation energy values range from 32 to 36 kJ mol^{-1}, which is higher than that of NafionÒ 117 membranes (12.75 kJ mol^{-1} [48]) and some organic-inorganic composite anion exchange membrane [49-51]. It can be deduced that both the ratio of hydrophilic/hydrophobic ((QCS+$G_{8\text{-}2\text{-}8}$)/PS) and the semi-IPN structure are responsible for the hydroxide anions conduction of the semi-IPN membranes and it is expected that the semi-IPN membranes would be more favorable in the higher temperature.

Methanol Permeability and Selectivity

The increasing content of $G_{8\text{-}2\text{-}8}$ means the increase in the content of linear block polymers which will result in an increase in the number of hydrophobic benzene rings on the block polymer and this could squeeze the OH^- transport

Table 2. IEC values and OH^- conductivities of M-X membrane in this work and literatures

Membrane	IEC (mmol·g^{-1})	Temp (°C)	Conductivity (10^{-3} S·cm^{-1})	Conductivity/IEC	Ref
PDCP-1.00-Im	1.86	30	27	14.5	39
DMBP-QTB	0.82	30	21	25.6	40
Quaternized poly(ether-imide)	0.98	30	2.3	2.3	41
QPAE	0.87	20	5.6	6.4	42
c6PAES-4IM-2.2	2.20	20	3.8	1.7	43
$G_{16\text{-}2\text{-}16}$-NaSal/PSF	0.15	30	3.47	21.9	44
QPVA/5 wt%GA	0.41	30	1.2	2.9	45
M-6	1.30	30	29.5	22.7	This work
M-30	1.49	30	81.9	54.9	This work

channels which will not only hinder the passage of methanol molecules, but also make the OH^- conduction more orderly, this could also be confirmed by the decreased Ea values form Figure 6. At the same time, the increasing content of linear block copolymer will make a more compact structure of semi-IPN which will help to inhibit the increase in methanol permeability.

As the anion exchange membrane in direct methanol fuel cell (DMFC) can act as a separator for OH^- and methanol, the selectivity was investigated as an index in order to evaluate the efficiency of the composite membrane in separating the two components (OH^- and methanol). The OH^-/methanol selectivity (*SP*) can be expressed in terms of $SP=\sigma/P$, i.e., the ratio of OH^- conductivity (σ) to methanol permeability (P), if OH^- flux and methanol flux are described using Fick's law and Nernst of Planck's equation, respectively. As can be seen in Table 3, with the increase in $G_{8\text{-}2\text{-}8}$ content, the methanol permeability of the composite membranes prepared in this work decreased from 4.51×10^{-6} $cm^{-2}\cdot s^{-1}$ to 3.23×10^{-6} $cm^{-2}\cdot s^{-1}$, this may be due to the fact that the semi-interpenetrating network structure of the composite membrane became more compact with the increasing content of linear block polymer which inhibited the permeation of methanol molecules. But, even the M-30 membrane with the lowest methanol permeability of 3.23×10^{-6} $cm^{-2}\cdot s^{-1}$ was higher than the commercial Nafion-115 membrane of 2.42×10^{-6} $cm^{-2}\cdot s^{-1}$. Therefore, further improvements on AEMs are needed. However, it is worth mentioning that the prepared composite membranes shows higher selectivities, take M-30 membrane as example, the selectivity is 25.3, while the Nafion-115 is 11.6, this is because M-30 membrane possesses a high OH^- conductivity of 8.19×10^{-2} $S\cdot cm^{-1}$ which is largely due to orderly arrangement of cationic groups on the linear block polymers making OH^- migration more effectively.

Alkaline Stability

Alkaline stability is a major concern for polymer electrolyte membranes applied in AEMFCs. In order to test whether the structure of the composite membrane changes before and after alkaline treatment, M-30 membrane with the highest OH^- conductivity was taken as test sample to investigate its FT-IR spectra after immersing in 1 M KOH aqueous solution at 80 °C. As can be seen in Figure 7, the absorption peak intensity of $-NR_3^+$ at 1480 cm^{-1} decreased and both the absorption peak intensity at 3435 cm^{-1} and 1250 cm^{-1} which were attributed to the -OH group and C-O group, respectively, increased by the extension of immersion time, indicating the degradation of quaternary ammonium groups. However, it is worth mentioning that the decline was not significant which was attributed to the formation of semi-IPN structure that improved the membrane alkaline stability.

Table 3. Properties of M-X membranes (X=6, 12, 18, 24, 30)

Membrane	IEC ($mmol\cdot g^{-1}$)	OH^- conductivity at 70 °C (10^{-2} $S\cdot cm^{-1}$)	Methanol permeation (10^{-6} $cm^{-2}\cdot s^{-1}$)	*SP*[a] (10^3 $S\cdot s\cdot cm^{-3}$)
QCS	1.17	0.69	3.68	1.9
M-6	1.30±0.12	2.95	4.51	6.5
M-12	1.37±0.09	3.89	4.22	9.2
M-18	1.42±0.10	5.07	4.13	12.2
M-24	1.46±0.07	6.38	3.44	18.5
M-30	1.49±0.11	8.19	3.23	25.3
Nafion®115	0.89-0.95	2.8	2.42	11.6

[a]*SP* selectivity parameter (*SP*) of conductivity at 70 °C and methanol permeation at room temperature measured in this work.

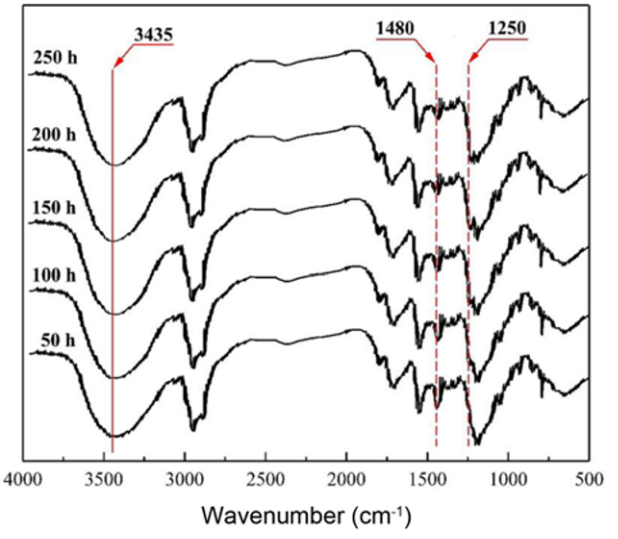

Figure 7. FT-IR spectra of M-30 membrane with different immersion time in 1 M KOH aqueous solution at 80 °C.

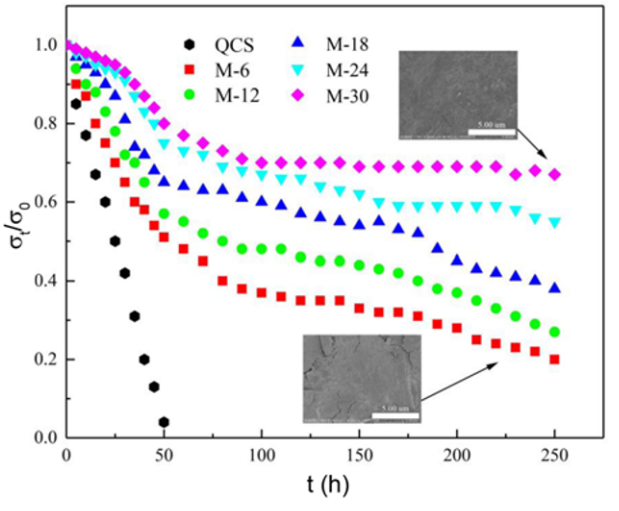

Figure 8. Alkaline stability of the M-X (X=6, 12, 18, 24, 30) membranes in alkaline solutions.

To investigate the tolerance of the M-X (X=6, 12, 18, 24 and 30) membranes in alkaline environments, the change of OH^- conductivity at 80 °C was monitored with immersion time in 1 M aqueous KOH solutions. The result was showed in Figure 8. As can be seen in Figure 8, the trend was noted which the conductivity initially decreased sharply and then stabilized over longer immersion time. As for the reason of conductivity, decreased sharply at the beginning of immersion was mainly due to the degradation of quaternary ammonium groups which come from QCS and $G_{8\text{-}2\text{-}8}$.

Especially, in the first 50 h, the composite membrane degradation was due to the displacement of the ammonium groups with OH^- anions via direct nucleophillic displacement and/or Hofmann elimination reaction when α, β hydrogen atoms and α carbon atoms are present. In the present work, there were α, β hydrogen atoms and α carbon atoms around the quaternary ammonium groups of QCS, and the direct nucleophilic displacement and Hofmann elimination reaction on the quaternary ammonium salt functionalized AEMs could not be eliminated. Thus, the OH^- conductivities of the membranes decreased sharply at the beginning of the alkaline immersion test. However, it was worthwhile to mention that the degradation on the conductivities of the M-X membranes with St-$G_{8\text{-}2\text{-}8}$ block polymers was near to stabilize after the immersion time was more than 50 h. It also can be seen in Figure 8, the M-6 and M-30 composite membranes exhibited different morphologies after immersing in alkaline solutions. Large part of cracks was observed on the surface of M-6 membrane revealing that the structure of M-6 membrane was hardly damaged in alkaline environment. However, only slight cracks can be found on the M-30 composite's surface, M-30 maintained a better membrane integrity exhibiting a better alkaline stability. This is due to the fact that M-30 composite membrane processes a denser semi-IPN structure and higher content of hydrophobic benzene rings and alkyl chains, which could inhibit the erosion of lye. This also can be confirmed by Figure 4. Hence, a better alkaline stability can be achieved and this is consistent with the trend of OH^- conductivity variation in alkaline environment.

Single Cell Performance

Figure 9 shows the variations in cell polarization and power density at 30 °C and 80 °C. The M-30 membrane with the highest OH^- conductivity and the aqueous solution with 5.0 M KOH combing 3.0 M ethanol were used in the cell performance tests. As can be seen from Figure 9, the cell performance is improved with increasing operating temperature. The open circuit potentials (OCPs) of single cell at 30 °C and 80 °C are 0.68 V and 0.76 V, respectively. The peak power density increase from 31 $mW \cdot cm^{-2}$ at 30 °C to 47 $mW \cdot cm^{-2}$ at 80 °C, which shows much better performance than the corresponding values in literatures [52] and the corresponding values in above literatures are usually lower than 20 $mW \cdot cm^{-2}$, which may be corresponded to its lower stability above 60 °C. The improved cell performance at an elevated operating temperature is mainly attributed to the following reasons. A higher operating temperature leads to quicker kinetics of both the ethanol oxidation and oxygen reduction which accelerates the electrochemical reaction rate. A raised temperature also increases the OH^- conductivity of membrane, which can be confirmed in Figure 5. Although the cell performance by using our membrane mentioned above is still lower than that of using commercial anion exchange membrane [53], the cell performance of the M-30 membrane (31 $mW \cdot cm^{-2}$ at 30 °C) is encouraging as compared with the open literature (8 $mW \cdot cm^{-2}$ at 30 °C) [54]. Our investigation to anion exchange membrane is still underway to further improve the performance of AEMFC.

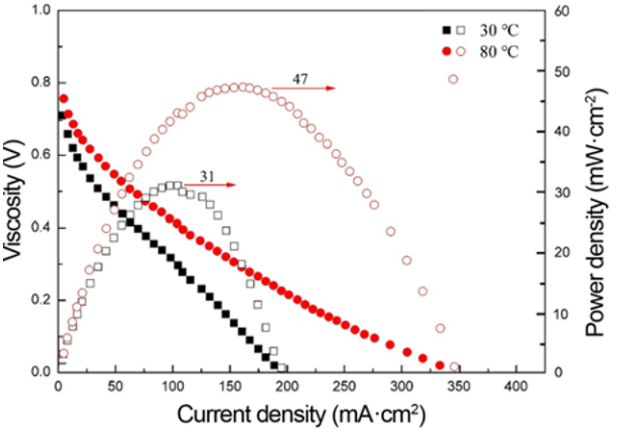

Figure 9. Polarization curves and power density curves of the M-30 membrane under operating temperature 30 °C and 80 °C.

Conclusion

In this work, we prepared a series of semi-IPN anion exchange membranes via in-situ polymerization by Styrene (St) and $G_{8\text{-}2\text{-}8}$ in QCS as matrix. The linear block polymers (St-$G_{8\text{-}2\text{-}8}$) of Styrene and $G_{8\text{-}2\text{-}8}$ was constructed which makes an order arrangement of quaternary ammonium groups improving the OH^- migration efficiency. The M-30 composite membrane performs a high OH^- conductivity of 8.20×10^{-2} $S \cdot cm^{-1}$ at 70 °C, the methanol permeability is 3.23×10^{-6} $cm^{-2} \cdot s^{-1}$ which is still lower than Nafion 115 of 2.42×10^{-6} $cm^{-2} \cdot s^{-1}$ at 70 °C, but shows a higher selectivity of 25.3 than Nafion of 11.6. Besides, the membranes exhibited excellent thermal stability (≥150 °C), the tensile strength of the composite membrane is in the range of 14-25 MPa and elongation at break is in the range of 16-37 % at room temperature, as well as superior chemical stability in 1.0 M KOH solution for 250 h showing a potential application in fuel cells.

Acknowledgments

We are grateful for the financial supports by the Scientific Research Fund of Liaoning Provincial Education Department (L2013153), Fundamental Research Funds for the Doctoral of Liaoning Provincial Natural Science Foundation (20141126), Science and Technology Development Fund Project of Fushun city (20141115) and Scientific Research Cultivation Fund of LSHU.

References

1. M. Z. Jacobson, W. G. Colella, and D. M. Golden, *Science*, **308**, 1901 (2005).
2. A. K. Mishra, S. Bose, and T. Kuila, *Prog. Polym. Sci.*, **37**, 842 (2012).
3. G. H. He, A. Li, and J. Zhao, *Adv. Mater.*, **27**, 5280 (2015).
4. N. Awang, A. F. Ismail, and J. Jaafar, *React. Funct. Polym.*, **86**, 248 (2015).
5. Y. J. Wang, J. L. Qiao, and R. Baker, *Chemical Society Reviews*, **42**, 5768 (2013).
6. J. R. Varcoe, P. Atanassov, and D. R. Dekel, *Energy. Environ. Sci.*, **7**, 3135 (2014).
7. S. Lu, J. Pan, and A. Huang, *China Basic Science*, **105**, 20611 (2009).
8. J. R. Varcoe and R. C. T. Slade, *Fuel Cells*, **5**, 187 (2005).
9. K. Asazawa, K. Yamada, and H. Tanaka, *Angew. Chem. Int. Edit.*, **46**, 8024 (2007).
10. S. C. Price, X. Ren, and A. C. Jackson, *Macromolecules*, **46**, 7332 (2013).
11. J. Yan and M. A. Hickner, *Macromolecules*, **43**, 2349 (2010).
12. Z. Zhang, K. Shen, and L. Lin, *J. Membr. Sci.*, **497**, 318 (2016).
13. D. S. Kim, C. H. Fujimoto, and M. R. Hibbs, *Macromolecules*, **46**, 7826 (2013).
14. L. Liu, Q. Li, and J. Dai, *J. Membr. Sci*., **453**, 52 (2014).
15. K. M. Hugar, H. A. K. Iv, and G. W. Coates, *J. Am. Chem. Soc*., **137**, 8730 (2015).
16. Y. Z. Zhuo, A. N. Lai, and Q. G. Zhang, *J. Mater. Chem. A*, **3**, 18105 (2015).
17. B. Zhang, S. Gu, and J. Wang, *Rsc Adv.*, **2**, 12683 (2012).
18. K. J. T. Noonan, K. M. Hugar, and H. A. K. Iv, *J. Am. Chem. Soc*., **134**, 18161 (2012).
19. S. Gu, R. Cai, and T. Luo, *Angew. Chem. Int. Edit.*, **48**, 6499 (2009).
20. Y. Zha, M. L. Disabbmille, and Z. D. Johnson, *J. Am. Chem. Soc*., **134**, 4493 (2012).
21. S. Gu, J. Wang, and R. B. Kaspar, *Scientific Reports*, **5**, 11668 (2015).
22. A. Weiber, D. Meis, and P. Jannasch, *Polym. Chem.*, **6**, 1986 (2015).
23. L. Lin, Y. Chen, G. Li, J. Gao, and K. Wu, *J. Power Sources*, **195**, 2212 (2010).
24. J. Zhou, M. Unlu, and J. A. Vega, *J. Power Sources*, **190**, 285 (2009).
25. Y. H. Wu, C. M. Wu, T. W. Xu, F. Yu, and Y. X. Fu, *J. Membr. Sci*., **321**, 299 (2008).
26. S. D. Lim, J. M. Rhee, C. Nah, S. H. Lee, and M. Y. Lyu, *Carbohydr. Res.*, **339**, 313 (2004).
27. J. Wu, Z. G. Su, and G. H. Ma, *Int. Phar.*, **315**, 1 (2006) .
28. R. H. He, Q. F. Li, A. Bach, A. O. Jensen, and N. J. Bjerrum, *J. Membr. Sci.*, **277**, 38 (2006).
29. M. R. Hibb, M. A. Hickner, T. M. Alam, S. K. Mcintyre, C. H. Fujimoto, and C. J. Cornelius, *Chem. Mater.*, **20**, 2566 (2008).
30. J. L. Wang, R. H. He, and Q. T. Che, *J. Colloid Interface Sci.*, **361**, 219 (2011).
31. J. L. Wang, Q. T. Che, and R. H. He, *J. Electrochem. Soc.*, **160**, F168 (2013).
32. J. H. Wang, S. H. Li, and S. B. Zhang, *Macromolecules*, **43**, 3890 (2010).
33. J. Ran, L. Wu, J. R. Varcoe, A. L. Ong, D. Poynton, and T. W. Xu, *J. Membr. Sci.*, **415-416**, 242 (2012).
34. J. L. Wang and L. L. Wang, *Solid State Ionics*, **255**, 96 (2014).
35. Y. Wan, B. Peppley, K. A. M. Creber, and V. T. Bui, *J. Power Sources*, **195**, 3785 (2010).
36. C. A. Ferreira, J. Casanovas, M. A. S. Rodrigues, F. Muller, E. Armelin, and C. Aleman, *J. Chem. Eng. Data*, **55**, 4801 (2010).
37. W. Mabrouka, L. Ogiera, F. Matoussic, C. Sollogoub, S. Vidala, M. Dachraouic, and J. F. Fauvarque, *Mater. Chem. Phys.*, **128**, 456 (2011).
38. Y. B. Wang, D. Yang, X. H. Zheng, Z. Y. Jiang, and J. Li, *J. Power Sources*, **183**, 454 (2008).
39. J. Pan, C. Chen, and Y. Li, *Energy. Environ. Sci.*, **7**, 354 (2013).
40. P. Zuo, Y. Su, and W. Li, *Macromol. Rapid Comm.*, **37**, 1748 (2016).
41. Z. Yang and R. Guo, *Angew. Chem. Int. Edit.*, **55**, 11499 (2016).
42. G. Wang, Y. Weng, and D. Chu, *J. Membr. Sci*., **326**, 4 (2009).
43. X. Li, Q. Liu, and Y. Yu, *J. Mater. Chem. A*, **1**, 4324 (2013).
44. E. A. Weiber and P. Jannasch, *J. Membr. Sci*., **520**, 425 (2016).
45. Y. F. Wang, H. T. Wan, and J. L. Wang, *J. Electrochem. Soc*., **164**, F1051 (2017).
46. C. C. Yang, S. S. Chiu, and S. C. Kuo, *J. Power Sources*, **199**, 37 (2012).
47. A. Roy, M. A. Hickner, X. Yu, Y. X. Li, T. E. Glass, and J. E. McGrath, *J. Polym. Sci., Part B: Polym. Phys.*, **44**, 2226 (2006).
48. D. Y. Chen and M. A. Hickner, *ACS Appl. Mater. Inter.*, **4**, 5775 (2012).
49. M. R. Hibbs, C. H. Fujimoto, and C. J. Cornelius,

Macromolecules, **42**, 8316 (2009).
50. J. R. Varcoe, R. T. C. Slade, E. L. H. Yee, S. D. Poynton, D. J. Driscoll, and D. C. Apperley, *Chem. Mater.*, **19**, 2686 (2007).
51. J. Yan and M. A. Hickner, *Macromolecules*, **43**, 2349 (2010).
52. A. Verma, A. K. Jha, and S. Basu, *J. Power Sources*, **141**, 30 (2005).
53. V. Bambagioni, C. Bianchini, A. Marchionni, J. Filippi, F. Vizza, and J. Teddy, *J. Power Sources*, **190**, 241 (2009).
54. C. C. Yang, Y. J. Li, S. J. Chiu, and K. T. Lee, *J. Power Sources*, **184**, 95 (2008).